Eur. Phys. J. C manuscript No.
(will be inserted by the editor)

Characterization of relativistic heavy-ion collisions at the Large Hadron Collider through temperature fluctuations

Sumit Basu[a,1] **Rupa Chatterjee**[1] **Bastanta K. Nandi**[2], **Tapan K. Nayak**[1]

[1]Variable Energy Cyclotron Centre, Kolkata - 700064, India
[2]Indian Institute of Technology Bombay, Mumbai - 400076, India

Received: date / Accepted: date

Abstract We propose to characterize heavy-ion collisions at ultra-relativistic energies by using fluctuations of energy density and temperature. Temperature fluctuations on an event-by-event basis have been studied both in terms of global temperature of the event, and locally by constructing fluctuation maps in small phase space bins in each event. Global temperature fluctuations provide an estimation of the specific heat of the system. Local temperature fluctuations of the event may be ascribed to the remnants of initial energy density fluctuations. Together these two observables give an insight into the system created in heavy-ion collisions and its evolution. Event-by-event hydrodynamic calculations indeed provide adequate theoretical basis for understanding the origin of the fluctuations. We demonstrate the feasibility of studying global and local temperature fluctuations at the Large Hadron Collider energy by the use of AMPT event generator.

PACS 25.75.-q,25.75.Nq,12.38.Mh

Keywords Quark-Gluon Plasma, hydrodynamics, correlations, fluctuations, heat capacity

1 Introduction

Heavy-ion collisions at ultra-relativistic energies create matter at extreme conditions of energy density (ϵ) and temperature (T), similar to the ones that existed within a few microseconds after the Big Bang [1]. The fireball produced in the collision goes through a rapid evolution from an early partonic phase of deconfined quark-gluon plasma (QGP) to a hadronic phase and ultimately freezing out after a few tens of fm. The major goals of colliding heavy-ions at the Relativistic Heavy Ion Collider (RHIC) and at the Large Hadron Collider (LHC) are to study the nature of the phase transition and understand the QGP matter in detail. With the production of large number of particles in each of the collisions, it has become possible to extract thermodynamic quantities on an event-by-event basis, rather than averaging over a sample of events. Event-by-event fluctuations of ϵ, T, mean transverse momentum, particle multiplicity, particle ratios, etc., as well as fluctuations of conserved quantities within finite detector acceptances have been proposed to provide dynamical information regarding the evolving system [2,3,4,5,6,7,8,9,10,11,12].

In this manuscript, temperature fluctuations have been studied on an event-by-event basis by estimating global temperature of the event, and local temperatures in small phase space bins within the event. Determination of temperature and its fluctuation for heavy-ion collisions have been possible because of large number of particles emitted in each event [13,14], which is essential to keep the statistical uncertainties of the measurements within a reasonable limit. Global event to event temperature fluctuations provide the heat capacity (C), which is an important thermodynamic quantity in characterizing the system. Lattice QCD calculations predict a strong temperature dependence of the heat capacity, the nature of which depends on the order of the phase transition [4,15]. This study sheds light on the nature of phase transition at the LHC energy. Fluctuations of initial energy density and temperature may survive till the freeze-out and manifest themselves in the measured temperature fluctuations. In fact, initial fluctuating conditions have been found to be necessary for explaining observed elliptic flow in central collisions and substantial triangular flow of charged particles [16]. The initial state fluctuations may have their imprint on

[a]e-mail: sumit.basu@cern.ch

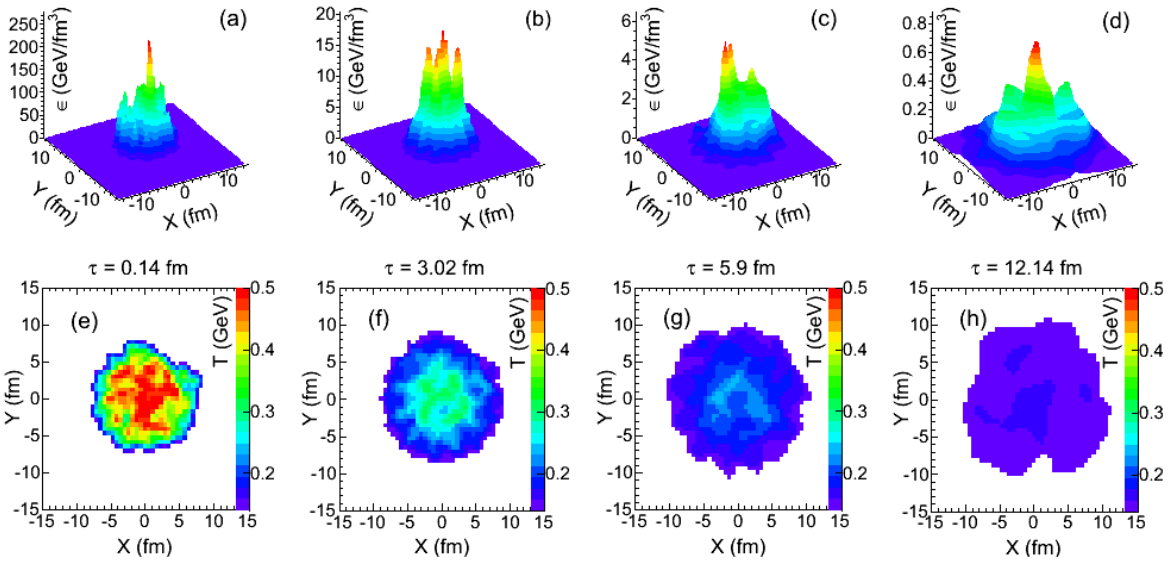

Fig. 1 (Color online). Distributions of energy density (upper panles) and temperature (lower panels) in the transverse (X-Y) plane at four proper times (τ) obtained from hydrodynamic calculations for a single central Pb-Pb event at $\sqrt{s_{\rm NN}}$ =2.76 TeV.

the bin to bin local fluctuations within an event. Event-by-event hydrodynamic calculations provide a strong theoretical basis for studying the global and local temperature fluctuations.

2 Event-by-Event hydrodynamical approach

Local fluctuations in energy density arise because of the internal structures of the colliding nuclei. These initial fluctuations manifest into local temperature fluctuations of the fireball at different stages of the collision. Relativistic hydrodynamic calculations which take such effects into account reveal large local fluctuations in ϵ and T in small phase space bins at early stages of the collision [1,16,17,18]. The local fluctuations have been quantified throughout the evolution by simulating central (0–5% of the total cross section) Pb-Pb events at $\sqrt{s_{\rm NN}}$ = 2.76 TeV by the use of a (2+1)-dimensional event-by-event ideal hydrodynamical framework [16] with lattice-based equation of state [19]. The formation time of the plasma is taken to be 0.14 fm [20,21]. A wounded nucleon (WN) profile is considered where the initial entropy density is distributed using a 2-dimensional Gaussian distribution function,

$$s(X,Y) = \frac{K}{2\pi\sigma^2} \sum_{i=1}^{N_{\rm WN}} \exp\Big(-\frac{(X-X_i)^2+(Y-Y_i)^2}{2\sigma^2}\Big) \quad (1)$$

Here X_i, Y_i are the transverse coordinates of the $i^{\rm th}$ nucleon and K is an overall normalization constant. The size of the density fluctuations is determined by the free parameter σ, which is taken to be 0.4 fm [16]. The transition temperature from the QGP to the hadronic phase is chosen to be 170 MeV and the kinetic freeze-out temperature is taken as 160 MeV. The results for ϵ and T at different times (τ) are analyzed for each collision in X-Y phase space bins in the transverse plane (each bin is chosen to be 0.6 fm×0.6 fm).

Time evolutions of the distributions of ϵ and T have been presented for four values of τ in Fig. 1 for a single event. The upper panels (a-d) of the figure show three dimensional view of ϵ, whereas the lower panels (e-h) show corresponding values of T in the transverse plane. At early times, sharp and pronounced peaks in ϵ and hotspots in T are observed. Large bin-to-bin fluctuations observed in ϵ and T indicate that the system formed immediately after collision is quite inhomogeneous in phase space. As time elapses, the system cools, expands, and the bin-to-bin variations in ϵ and T smoothen out.

Observations from Fig. 1 have been quantified in terms of the mean energy density ($\langle\epsilon\rangle$), mean temperature ($\langle T\rangle$) over the X-Y bins, and the bin-to-bin fluctuations of ϵ and T as a function of τ. The time evolution of $\langle\epsilon\rangle$, $\langle T\rangle$, and their fluctuations are presented in Fig. 2, where τ is plotted in logarithmic scale for zooming in on the early times. The shaded regions represent the extent of event-by-event variations, taken from a sample of five hundred events. It is observed that $\langle\epsilon\rangle$ falls sharply from ∼168 GeV/fm^3 at $\tau = 0.14$ fm to a value of ∼20 GeV/fm^3 at τ = 1 fm, and then falls slowly till freeze-out. The initial ϵ is close to the experimental

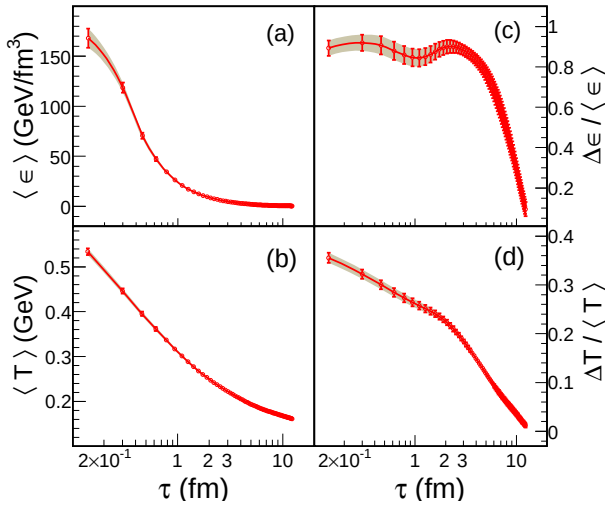

Fig. 2 (Color online). Temporal evolution of (a) average energy density, (b) average temperature, (c) fluctuations in energy density, and (d) fluctuations in temperature for central Pb-Pb collisions at $\sqrt{s_{\rm NN}}$ =2.76 TeV, obtained from hydrodynamic calculations. Averaging is taken over the X-Y bins in every event. The shaded regions represent the extent of event-by-event variations for a large number of events.

result, estimated by the ALICE collaboration [13,22]. The fall of $\langle T\rangle$ with τ is smooth, which goes down from ∼530 MeV at $\tau = 0.14$ fm to ∼300 MeV at $\tau = 1$ fm. At the freeze-out, as expected, $\langle T\rangle$ is close to 160 MeV.

The bin-to-bin fluctuations, $\Delta\epsilon/\langle\epsilon\rangle$ and $\Delta T/\langle T\rangle$, are presented in the right panels of Fig. 2, where $\Delta\epsilon$ and ΔT are the root mean square (RMS) deviations of the two quantities over the bins. At early times, the fluctuations are observed to be very large (∼90% and ∼35% for ϵ and T, respectively), which indicate the violent nature of the matter created in the collision. Interestingly, although $\langle\epsilon\rangle$ decreases quite fast, the fluctuation in ϵ remains almost constant up to τ∼2.5 fm, and then decreases rapidly. Around the same τ, the fluctuation in T shows a kink, beyond which the fluctuation decreases even faster. During the hydrodynamic evolution, there may be a characteristic change in the behaviour of the system at this time, which needs to be understood. Nevertheless, it is clear that a detailed insight to the evolution of fluctuations is possible by studying local temperature fluctuations.

3 Global Temperature Fluctuations

Fluctuations of any observable of a system have two distinct origins, first, quantum fluctuations which are initial state fluctuations occurring at fast time scales and second, classical thermodynamical fluctuations which occur after elapse of sufficient time after the collision [23, 24]. Initial state fluctuations arise because of internal structures of the colliding nuclei, and fluctuation in initial energy densities, and appear as event-by-event fluctuations in the energy density or temperature. Thermodynamic fluctuations have multiple sources, such as local thermal fluctuations of energy density, and event-by-event variation in the freeze-out conditions. Fluctuations of these observables are related to several thermodynamic parameters. For example, fluctuation in temperature are related to the heat capacity of the system [2,23]:

$$\frac{1}{C} = \frac{(\Delta T^2)}{T^2}, \tag{2}$$

where T is the temperature of the system at freeze-out[1], and $\Delta T^2 = \langle T^2\rangle - \langle T\rangle^2$.

Fluctuations in a thermodynamic quantity like temperature may arise due to fluctuations in energy or entropy or finite particle number, and can be calculated from $\langle p_{\rm T}\rangle$ (mean transverse momentum) fluctuations or $p_{\rm T}$ correlations [4,5,6,25,26,27,28,29]. However, according to Ref. [5], variation of C is similar to fluctuation in energy rather than the $p_{\rm T}$ fluctuation. Thus $p_{\rm T}$ correlation is not an appropriate measure of the temperature fluctuation, and may also affect measurement of C. To circumvent this limitation, we have come up with a new approach by assigning a temperature to an event and estimating event-by-event fluctuation for a given class of events. In fact, for central Pb-Pb collisions at the LHC energy, large number of produced particles in each event form a well defined exponential distribution in $p_{\rm T}$. The inverse slope parameter of the distribution gives the effective temperature, and subsequently, the heat capacity of the system can be calculated by using eqn. (2).

A feasibility study of calculating the global event temperature and local temperatures in small phase space bins has been made for Pb-Pb collisions at $\sqrt{s_{\rm NN}} = 2.76$ TeV, corresponding to the LHC energy. The string melting (SM) mode of the AMPT model [32] has been employed, which mimics the experimental conditions. This mode of AMPT model, using parameter set-B as given in Ref. [36,37], includes a fully partonic phase that hadronizes through quark coalescence, and has been shown to reproduce the experimental data at LHC energy [35,36,37,38].

A large number of particles produced in every central Pb-Pb collisions at $\sqrt{s_{\rm NN}}$ =2.76 TeV makes it possible to construct $m_{\rm T}$ spectra of identified particles in

[1] For part of a thermodynamically equilibrated system with fluctuating energy (E), the heat capacity [5] can be expressed through $(\Delta E^2) = T^2C(T)$. This can be applied for a locally thermalized system produced during the evolution of heavy-ion collisions.

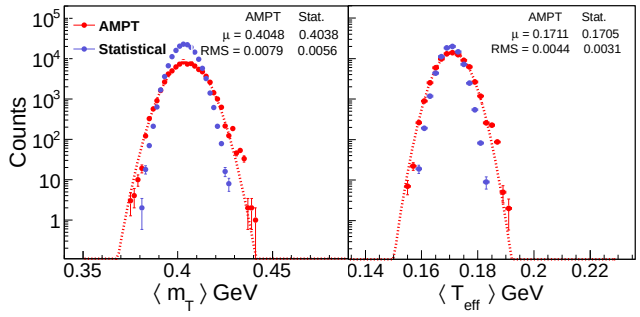

Fig. 3 (Color online). Event-by-event distribution of $\langle m_{\rm T}\rangle$ and corresponding $T_{\rm eff}$ for pions within one unit of rapidity and full azimuth for central Pb-Pb collisions at $\sqrt{s_{\rm NN}}$ = 2.76 TeV using AMPT. Distributions for synthetic events representing the statistical component are overlaid on the figure.

every event. Fitting the $m_{\rm T}$ distribution of pions with a Maxwell-Boltzmann distribution yields the value of the effective temperature, $T_{\rm eff}$ in each event. This temperature is related to the $\langle m_{\rm T}\rangle$ of pions within a given acceptance:

$$\langle m_{\rm T}\rangle = \frac{2T_{\rm eff}^2 + 2m_0T_{\rm eff} + m_0^2}{m_0 + T_{\rm eff}}, \tag{3}$$

where m_0 is the mass of pions. From the AMPT events, it is verified that for pions within the central rapidity ($-0.5 \leq y \leq 0.5$), full azimuth and $m_0 \leq m_{\rm T} \leq 1.5$ GeV, the value of $T_{\rm eff}$ from fitting the $m_{\rm T}$ spectrum as well as from $\langle m_{\rm T}\rangle$ are similar to each other. The upper limit of $m_{\rm T}$ is chosen to exclude pions, which may be affected by jets. Figure 3 shows the distributions of $\langle m_{\rm T}\rangle$ of pions and corresponding values of $T_{\rm eff}$ calculated using the above expression for a large number of events. It should be noted that the values of $T_{\rm eff}$ have contributions from both a thermal part ($T_{\rm kin}$) and a second component which depends on the collective transverse velocity ($\langle\beta_{\rm T}\rangle$) of the system such that $T_{\rm eff} = T_{\rm kin} + f(\beta_{\rm T})$. For pions, $f(\beta_{\rm T}) \approx m_0\langle\beta_{\rm T}\rangle^2$ [33]. For top central (0-5%) collisions, the transverse velocity can be assumed to be same for all events due to spherical symmetry, and the fluctuations in the flow velocity can be neglected [5]. Thus the fluctuation in $T_{\rm eff}$ may be a good representation of the fluctuation in temperature, ($\Delta T_{\rm kin} = \Delta T_{\rm eff}$). Being a thermodynamic quantity, the heat capacity is only connected to $T_{\rm kin}$, and eqn. 2 can be rewritten as:

$$\frac{1}{C} = \frac{(\Delta T_{\rm kin}^2)}{T_{\rm kin}^2} \approx \frac{(\Delta T_{\rm eff}^2)}{T_{\rm kin}^2}. \tag{4}$$

Event-by-event global temperature fluctuation has contributions from both the statistical and dynamical components. The statistical component arises due to limited number of particle production in heavy-ion collisions, and does not contribute to the measurement of heat capacity of the system. Statistical component of the fluctuation has been estimated by constructing randomly generated "synthetic" events, keeping the multiplicity and $p_{\rm T}$ distributions similar to those of the AMPT events. The $\langle m_{\rm T}\rangle$ and $T_{\rm eff}$ distributions of the synthetic events are also shown in Fig. 3. The dynamical component of the global temperature fluctuation, obtained by subtracting the statistical component of the fluctuation from the total, has been estimated to be $\Delta T_{\rm eff}$ = 3.12 MeV. According to Ref. [34], $T_{\rm kin}$ = 0.095 and $\langle\beta_{\rm T}\rangle$ = 0.651 from combined Blast Wave fits. This corresponds to heat capacity of C = 927.1.

Specific heat of the system is defined as heat capacity per volume at the thermodynamic limit. For ideal gas, specific heat is (3/2)N, where N is the Avogadro's number. For finite number of particles, the specific heat can be expressed as heat capacity per particle. We define the specific heat (c_v) as the heat capacity per pion multiplicity within the central rapidity ($-0.5 \leq y \leq 0.5$) and $0 \leq \phi \leq \pi$). The c_v is found to be 0.633. Considering the variation of β_T within 0.63 and 0.67 [34], the value of c_v turns out to be within the range of 0.594 to 0.687. This is the first estimation of c_v at LHC energies from model calculations.

4 Local Temperature Fluctuations

Local temperature fluctuations, which provide the amount of non-uniformity within a single event, are studied by dividing the available phase space into several y–ϕ bins, and estimating the bin temperature ($T_{\rm bin}$). It helps to find local hotspots created during the initial energy density, whether those have survived or died out. The bin temperatures are obtained using the similar prescription as above. The $\langle m_{\rm T}\rangle$ of pions are calculated within the y–ϕ bin and $m_0 \leq m_{\rm T} \leq 1.5$ GeV, and $T_{\rm bin}$ is evaluated by using eqn. (3). The number of y–ϕ bins has been chosen by taking into account the number of pions in each bin so that fluctuations in the number of pions do not affect the estimation of $m_{\rm T}$. The amount of local fluctuation may vary depending on the number of y bins, which needs to be evaluated.

For a given event, local temperature fluctuation in a given y–ϕ bin is expressed as:

$$F_{\rm bin} = (T_{\rm bin} - T_{\rm eff})/T_{\rm eff}. \tag{5}$$

For each event, a fluctuation map in y–ϕ phase space is constructed by plotting the corresponding values of $F_{\rm bin}$. Fig. 4 shows the the temperature fluctuation map for a typical event in 6×6 bins in y–ϕ, where the fluctuations are represented by different colour pallets. This map gives a quantitative view of the local temperature fluctuation in the available phase space for an event.

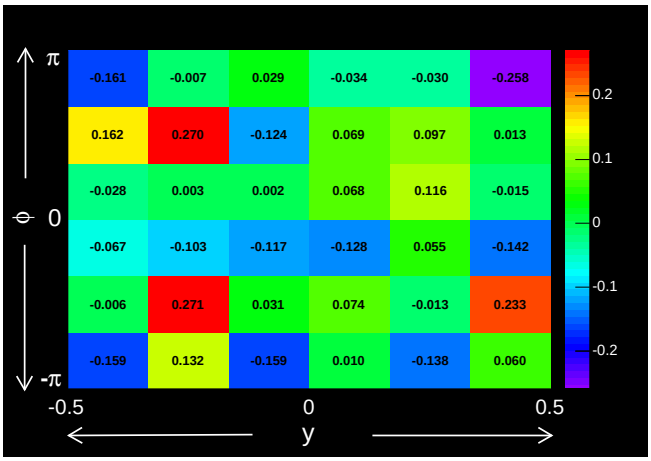

Fig. 4 (Color online). Temperature fluctuation map in y–ϕ bins for central Pb-Pb collisions at $\sqrt{s_{\rm NN}} = 2.76$ TeV using the AMPT model. For each y–ϕ bin, fluctuation is expressed as $(T_{\rm bin} - T_{\rm eff})/T_{\rm eff}$, the deviation of the bin temperature to the event temperature. The colour palettes indicate the magnitude of fluctuations.

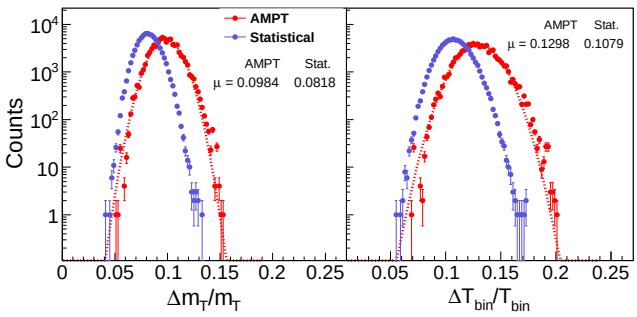

Fig. 5 (Color online). Event-by-event local temperature fluctuations, obtained from 6×6 y–ϕ bins in central rapidity and full azimuth for central Pb-Pb collisions at $\sqrt{s_{\rm NN}} = 2.76$ TeV using the AMPT event generator.

The map shows several hot (red) as well as cold (blue) zones, and zones with average (green) fluctuation throughout the phase space. It is to be seen whether the hot and cold zones have their origin from the extreme regions of phase space that existed during the early stages of the reaction.

For a single event, the amount of local temperature fluctuation is quantified by the ratio of RMS to the mean of the $T_{\rm bin}$ distribution. Local fluctuations in $\langle m_{\rm T} \rangle$ and corresponding temperature for each event have been evaluated and their event-by-event distributions are plotted in Fig. 5. The left and right panels of the figure show the distributions from $\langle m_{\rm T} \rangle$ and $T_{\rm bin}$, respectively. Mean value of the local temperature fluctuation for the event sample is 12.98% for 6×6 bins in central rapidity. Statistical component of the local fluctuations has been extracted from the "synthetic" events as discussed earlier. The mean value corresponding to the statistical component of the local temperature fluctuation has been estimated to be 10.79% as shown in Fig. 5. The average dynamical local fluctuation, extracted after subtracting the statistical component, for AMPT events is 7.2%. The non-zero value of local temperature fluctuation may imply that these might have the contributions from the early state fluctuations.

5 Remarks

Extraction of temperature fluctuations from experimental data maybe affected by some of the effects. Event plane orientation is one such effects, which needs to be taken care of, especially for non-central events. For the present study using AMPT, the events are event plane oriented. Fourier decomposition of the momentum distributions in the transverse plane yields a ϕ–independent, axially symmetric radial flow component and a ϕ–dependent part containing the anisotropic flow coefficients. For most central collisions, radial flow remains similar for all the events and the anisotropic flow components do not affect the slope of the $m_{\rm T}$ distribution. Final state effects, such as resonance decay, and hadronic rescattering tend to make the $m_{\rm T}$ spectra softer, and so choice of the $m_{\rm T}$ window has to be made in order to minimize such effects. Although present analysis uses charged pions, species dependence of temperature fluctuations may provide extra information regarding their freeze-out hyper surfaces as the particle production mechanisms of mesons, baryons and strange particles are different. This study may shed light on whether the origin of the temperature fluctuations are solely due to initial state fluctuations or includes final state effect. Viscosity tends to dilute the fluctuations. The SM version of AMPT includes the effect of viscosity ($\eta/s \sim 0.15$ at T=436 MeV [35,38]). Further analysis using a viscous hydrodynamic models will be more realistic for this study.

Local temperature fluctuation map for each event, as shown in Fig. 4, has a striking similarity to the fluctuation map of the cosmic microwave background radiation (CMBR) [39]. Fluctuation analysis of CMBR fluctuation map confirms the Big Bang evolution, inflation and provides information regarding the early Universe. The study of higher order moments using the maps may give access to various thermodynamic parameters at the early stages of the evolving system. Similarly, the fluctuation maps of heavy-ion collisions may form the basis of power spectrum analysis [40,41,42]. Access to large number of events in heavy-ion collisions compared to single event analysis in CMBR may have definite advantage which can be utilized to our advantage in or-

der to gain access to conditions that prevailed at the primordial state.

6 Summary

Event-by-event temperature fluctuations over full phase space as well as local phase space bins have been proposed to characterize the hot and dense system produced in heavy-ion collisions at ultra-relativistic energies. The global temperature fluctuations provide the heat capacity as well as specific heat of the system, whereas the observation of local fluctuations would imply the presence of fluctuations at early stages of the collision. Relativistic hydrodynamic calculations have been used to understand the evolution of ϵ and T fluctuations. It shows that the system exhibits fiercely large fluctuations at early times, which diminishes with the elapse of time.

The feasibility of studying temperature fluctuations in Pb-Pb collisions at $\sqrt{s_{\rm NN}}$=2.76 TeV has been demonstrated by using simulated events from the AMPT model. Temperatures are extracted from $\langle m_{\rm T} \rangle$ of charged pions. The global fluctuation in the event temperature has been extracted and used to calculate the heat capacity as $C = 927.1$. The specific heat per pion has been extracted to be $c_v = 0.633 \pm 0.054$ at the LHC energy, which is consistent with the results at RHIC energies [43]. At the LHC, the phase transition is expected to be a cross over. Thus the transition may not take place at a unique point in the phase diagram due to the evolution of entropy fluctuation created at the initial state, which reflects into energy density and temperature fluctuations. Thus, the estimation of the heat capacity helps in understanding the nature of the phase transition. The variation of c_v as a function of center-of-mass beam energy for Au+Au collisions at RHIC may provide an effective tool for locating the QCD critical point [30,31]. At LHC energies, it is possible to extract local temperatures over small phase space bins in central rapidity. Extraction of Local temperature fluctuation complements the global event temperature fluctuation as the origin of local fluctuations may be of primordial in nature. For the AMPT, local temperature fluctuations over small phase bins within each event have been extracted. The amount of local fluctuation is 7.2% for 6×6 bins in central rapidity. The observation of the non-zero local fluctuation may imply that a part of the initial fluctuations might have survived till freeze-out. The present study of global and local temperature fluctuations in conjunction with theoretical model calculations open up new avenues for characterizing the heavy-ion collisions.

Acknowledgements We would like to thank H. Holopainen for providing us with the event-by-event hydrodynamic code. This research used resources of the LHC grid computing facility at the Variable Energy Cyclotron Centre. SB is supported by the Department of Atomic Energy, Government of India.

References

1. U. Heinz, J. Phys.: Conf. Ser. **455**, 012044 (2013).
2. L. Stodolsky, Phys. Rev. Lett. **75**, 1044 (1995).
3. M.A. Stephanov, K. Rajagopal and E. V. Shuryak, Phys. Rev. Lett. **81**, 4816 (1998).
4. E.V. Shuryak, Phys. Lett. **B 423**, 9 (1998).
5. M.A. Stephanov, K. Rajagopal and E. V. Shuryak, Phys. Rev. **D 60**, 114028 (1999).
6. G. Wilk and Z. Wlodarczyk, Phys. Rev. Lett. **84**, 2770 (2000).
7. G. Wilk and Z. Wlodarczyk, Eur. Phys. Jour. **A 48**, 161 (2012).
8. T.K. Nayak, Jour. Phys. **G 32** S187 (2006).
9. S. Jeon and V. Koch, arXiv:hep-ph/0304012v1 (2003).
10. R. V. Gavai and Sourendu Gupta, Phys. Rev. **D 73**, 014004 (2006).
11. S. Borsanyi *et al.*, JHEP **1201** 138 (2012).
12. S. Ejiri, F. Karsch, K. Redlich, Phys. Lett. **B 633** 275 (2006).
13. K. Aamodt *et al.*, (ALICE Collaboration), Phys. Rev. Lett. **105**, 252301 (2010).
14. E. Abbas *et al.*, (ALICE Collaboration), Phys.Lett. **B 726** 610 (2013).
15. R. Gavai, S. Gupta and S. Mukherjee, Phys. Rev. **D 71**, 074013 (2005).
16. H. Holopainen, H. Niemi, and K. Eskola, Phys. Rev. **C 83**, 034901 (2011).
17. H. Song, arXiv:1401.0079v1 [nucl-th].
18. S. Floerchinger, U.A. Wiedemann, Phys. Rev. **C 88**, 044906 (2013).
19. M. Laine and Y. Schroder, Phys. Rev. **D 73**, 085009 (2006).
20. R. Paatelainen *et al.*, Phys. Rev. **C 87**, 044904 (2013).
21. R. Chatterjee *et al.*, Phys. Rev. **C 83**, 054908 (2011).
22. A. Toia (ALICE Collaboration), Jour. Phys. **G 38**, 124007 (2011).
23. L.D. Landau and I.M. Lifschitz, Course of Theoretical Physics, Statistical Physics Vol. 5 (Pergamon Press, New York, 1958).
24. J. I. Kapusta, B. Muller, and M. Stephanov, Phys.Rev. **C 85**, 054906 (2012)
25. R. Korus *et al.*, Phys. Rev. **C 64**, 054908 (2001).
26. S. Mrowczynski, Phys. Lett. **B 430**, 9 (1998).
27. S.A. Voloshin, V. Koch, and H.G. Ritter, Phys. Rev. **C 60** 024901 (1999).
28. T. Alber *et al.* (NA49 Collaboration) Phys. Rev. Lett. **75** 3814 (1995).
29. L. Adamczyk *et al.* (STAR Collaboration) Phys. Rev. **C 87**, 064902 (2013).
30. M.M. Aggarwal *et al.* (STAR Collaboration) arXiv:1007.2613 [nucl-ex] (2010).
31. R.V. Gavai, arXiv:1404.6615 [hep-ph] (2014).
32. Z.-W. Lin, C.M. Ko, B.-A. Li, B. Zhang, S. Pal, Phys. Rev. **C 72**, 064901 (2005).
33. J.K. Nayak and J. Alam, Phys. Rev. **C 80**, 064906 (2009).
34. B. Abelev *et al.* (ALICE Collaboration), Phys. Rev. **C 88**, 044910 (2013).

35. S. Pal and M. Bleicher, Phys. Lett. **B 709**, 82 (2012).
36. J. Xu and C.M. Ko, Phys. Rev. **C 83**, 034904 (2011).
37. J. Xu and C.M. Ko, Phys. Rev. **C 84**, 014903 (2011).
38. D. Solanki, *et al.*, Phys. Lett. **B 720**, 352 (2013).
39. E. Komatsu and C. L. Bennett (WMAP science team) Prog. Theor. Exp. Phys., 06B102 (2014).
40. A.P. Mishra *et al.*, Phys. Rev. **C 77**, 064902 (2008); *ibid.*, Phys. Rev. **C 81**, 034903 (2010).
41. A. Mocsy and P. Sorensen, Nucl. Phys. **A 855**, 241 (2011).
42. P. Naselsky *et al.* Phys. Rev. **C 86**, 024916 (2012).
43. Ben-Hao Sa *et al.* Phys. Rev. **C 75**, 054912 (2007).